Biochimica et Biophysica Acta 1840 (2014) 113–119

Contents lists available at ScienceDirect

Biochimica et Biophysica Acta

journal homepage: www.elsevier.com/locate/bbagen

Tracking sulfur and phosphorus within single starch granules using synchrotron X-ray microfluorescence mapping

Alain Buléon [a,*], Marine Cotte [b,c], Jean-Luc Putaux [d,1], Christophe d'Hulst [e], Jean Susini [b]

[a] INRA-UR 1268 BIA, Rue de la Géraudière, BP 71627, F-44316 Nantes cedex 3, France
[b] ESRF (European Synchrotron Radiation Facility), 6 rue Jules Horowitz, F-38000 Grenoble, France
[c] LAMS (Laboratoire d'Archéologie Moléculaire et Structurale) UMR-8220, 3 rue Galilée, 94200 Ivry-sur-Seine, France
[d] CERMAV-CNRS, BP 53, F-38041 Grenoble Cedex 9, France
[e] UGSF, UMR 8576 CNRS, Université Lille 1, Bât. C9, F-59655 Villeneuve d'Ascq Cedex, France

ARTICLE INFO

Article history:
Received 17 April 2013
Received in revised form 24 July 2013
Accepted 29 August 2013
Available online 7 September 2013

Keywords:
Micro X-ray fluorescence
Synchrotron
Starch
Sulfur
Phosphorus
Granule bound starch synthase

ABSTRACT

Background: Native starch accumulates as granules containing two glucose polymers: amylose and amylopectin. Phosphate (0.2–0.5%) and proteins (0.1–0.7%) are also present in some starches. Phosphate groups play a major role in starch metabolism while granule-bound starch synthase 1 (GBSS1) which represents up to 95% of the proteins bound to the granule is responsible for amylose biosynthesis.
Methods: Synchrotron micro-X-ray fluorescence (μXRF) was used for the first time for high-resolution mapping of GBSS1 and phosphate groups based on the XRF signal of sulfur (S) and phosphorus (P), respectively. Wild-type starches were studied as well as their related mutants lacking GBSS1 or starch-phosphorylating enzyme.
Results: Wild-type potato and maize starch exhibited high level of phosphorylation and high content of sulfur respectively when compared to mutant potato starch lacking glucan water dikinase (GWD) and mutant maize starch lacking GBSS1. Phosphate groups are mostly present at the periphery of wild-type potato starch granules, and spread all over the granule in the amylose-free mutant. P and S XRF were also measured within single small starch granules from *Arabidopsis* or *Chlamydomonas* not exceeding 3–5 μm in diameter.
Conclusions: Imaging GBSS1 (by S mapping) in potato starch sections showed that the antisense technique suppresses the expression of GBSS1 during biosynthesis. P mapping confirmed that amylose is mostly present in the center of the granule, which had been suggested before.
General significance: μXRF is a potentially powerful technique to analyze the minor constituents of starch and understand starch structure/properties or biosynthesis by the use of selected genetic backgrounds.

1. Introduction

Native starch, the major energy reserve of a large variety of higher plants, accumulates as a complex granular structure containing two distinct α-linked glucose polymers: quasi-linear amylose and moderately branched amylopectin. Amylopectin, the major fraction of starch, is thought to be the basis of the semicrystalline architecture of the granule while amylose is generally considered as an amorphous polymer [1,2]. The relative position of amylose and amylopectin within the granule is not known with certainty yet. Nevertheless, the synthesis of amylose occurs within the amylopectin matrix [3,4] and some reports suggest that amylose is preferably located at the hilum of the granule [5,6].

The size and shape of starch granules strongly depend on their origin with a size typically varying from 1 μm for amaranth to 50–60 μm for potato. Besides lipids, essentially contained in cereal starches, phosphate (0.2–0.5%) and proteins (0.1–0.7%) can be present in some starches depending on their origin [1,7]. Among the numerous enzymes involved in starch biosynthesis, granule-bound starch synthase 1 (GBSS1) is one of the various elongating enzymes (glycosyltransferases of the GT5 family of the CAZy classification; www.cazy.org) only responsible for amylose biosynthesis. GBSS1 naturally represents up to 95% of the proteins non-covalently bound to the granule where it is active. Depending on growth conditions, tissue origin, or genetic background, the GBSS1 content may reach 0.5% of the mass of the granule being by far the most represented protein within the starch granule. GBSS1-deficient starches lack not only the corresponding protein but also more or less completely the amylose fraction such as in *waxy* maize, [8] *amf* potato [9] or *lam* pea [10], for example.

Starch is also naturally phosphorylated on some of its glucose residues at C3 and C6 positions. It has been shown that most phosphate groups are bound to amylopectin but not to amylose [11,12]. Phosphate groups are present not only in amorphous regions but also in crystalline domains. Phosphorylation of starch is required to trigger polysaccharide catabolism by degrading enzymes [13]. Specialized enzymes are responsible for starch phosphorylation: glucan water dikinase (GWD)

* Corresponding author. Tel.: +33 2 40 67 50 47; fax: +33 2 40 67 50 43.
E-mail address: alain.buleon@nantes.inra.fr (A. Buléon).
[1] Affiliated with Université Joseph Fourier, member of Institut de Chimie Moléculaire de Grenoble and Institut Carnot PolyNat.

0304-4165/$ – see front matter © 2013 Elsevier B.V. All rights reserved.
http://dx.doi.org/10.1016/j.bbagen.2013.08.029

and phosphoglucan water dikinase (PWD) [14–16]. Like GBSS1, both enzymes are bound to the starch granule but represent only tiny amounts with respect to the total protein content (<5% of the proteins) present in the granule.

Analyzing the nature of minor components in starch is not trivial and locating them at high resolution is even more difficult, given the small size of the starch granule and small amounts of phosphorus and sulfur. Using particle-induced X-ray emission (PIXE), Blennow and co-workers [17] analyzed the content in P and other elements like K, Ca, Mg and Si in potato starch. Tawil et al. localized GBSS1 in maize starch using synchrotron UV microscopy [18].

Chlamydomonas reinhardtii (a unicellular eukaryotic green algae) and *Arabidopsis thaliana* (a model vascular dicot plant) have been successfully used as models to investigate the genetics of plant starch biosynthesis. *Chlamydomonas* is particularly useful to mimic different plant tissues depending on the growth conditions: storage organs when grown in nitrogen starvation (−N) (favoring non-cyclic high starch accumulation); photosynthetic tissues when grown in nitrogen-supplied medium (+N) (lower starch content submitted to recurrent synthesis/degradation cycles [19]). Several mutant strains defective for enzymes of the starch metabolic pathway have been isolated in *C. reinhardtii*. This genetic diversity provides a good access to a wide range of starch resources with specific features that were already characterized in details. This genetic diversity includes mutations for the synthesis of the precursor molecule of starch synthesis (*sta1*-; *sta6*-) [20,21], the synthesis of amylose (*sta2*-) [22], and the synthesis of amylopectin (*sta3*-, *sta7*-) [23,24]. A mutant strain defective for the plastidial isoform of starch-phosphorylase was also described for *Chlamydomonas* (mutant strain in locus *STA4*) with altered starch synthesis [25]. An additional interesting aspect of *Chlamydomonas* is that the GBSS1 and the amylose content within the starch granule can be controlled by the growth condition of the algae [26] and that the activity of the algal enzyme is 10-fold higher than that of orthologous enzymes in higher plants [4]. Thus, amylose synthesis can be easily managed in vitro by supplying ADP-glucose to individual intact starch granules [3,4].

Arabidopsis is also a powerful model to develop a reverse genetics approach and numerous genomics tools are available with this plant (http://arabidopsisbook.org). A wide range of mutants or transgenic lines with altered genotypes has been studied offering a large panel of starches with altered phosphate or protein contents or even starch granule size that can easily be associated to an enzyme/protein activity (for a review, see ref. [27]).

In the present work, we have analyzed sulfur (S mapping; this signal is mostly due to GBSS1) and phosphate (P mapping) groups by synchrotron-based X-ray fluorescence microscopy (μXRF) with high lateral resolution. The objective was to develop a reliable non-denaturing and non-intrusive approach to determine the distribution of the enzyme responsible for amylose synthesis (GBSS1) and to correlate this distribution with the relative organization of amylopectin and amylose within the starch granule. Wild-type (WT) *Arabidopsis* and *Chlamydomonas* starches were studied as well as their related mutants lacking GBSS1 or GWD proteins. This was a challenging task because of the very small size of the starch granules in these model plants (smaller than 5 μm of diameter for both organisms). Samples of maize and potato starch granules (WT or mutant or transgenic backgrounds when available) of a much larger size (up to several tens of μm in diameter) have been included in this work. Moreover, potato starch is known to be natively highly phosphorylated [28] which thus defines an ideal positive control for the experiments conducted in this work.

2. Experimental section

2.1. Starch sources

Wild-type potato and maize and waxy maize (Waxylis 100) starches were purchased from Roquette (Lestrem, France) (Fig. 1A,C). asGWD potato starch was a gift from A. Blennow (University of Copenhagen, Denmark). Potato starch sections (5 μm) were given by P. Mongondry (Engineer School of Agriculture Angers, France) (Fig. 1B). *C. reinhardtii* starch samples were prepared as described by Delrue et al. [22] after the cells were cultivated either under nitrogen starvation or under exponential growth condition (i.e., in a medium supplemented with a source of nitrogen), following Ball et al. [26] (Fig. 1D). *A. thaliana sex1-3* mutant starch samples were kindly provided by M. Steup (University of Potsdam, Germany) while *ss4*- mutant starch was prepared as described in Roldan et al. [29]. *C. reinhardtii* and *A. thaliana* samples were washed and centrifuged 4 times in water up to disappearance of any sulfonate and/or silicone XRF signal stemming from 3-(N-morpholino) propanesulfonic acid (MOPS) and/or Percoll used for extraction and purification. μXRF experiments were conducted on starch granules from maize, *C. reinhardtii* and *A. thaliana* and potato starch sections. Starch granules were suspended in water and deposited on a film of Ultralene (Spex CertiPrep). The suspension was allowed to dry before measurement and the quality of the preparation evaluated by light microscopy. Dry embedded potato starch sections were directly sandwiched between two Ultralene films.

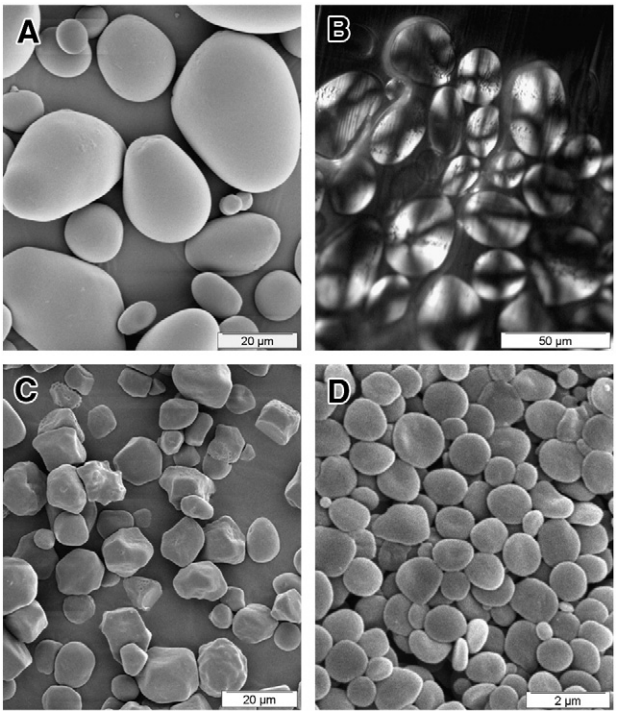

Fig. 1. Starch granules from wild-type potato (A, B), waxy maize (C) and wild-type *Chlamydomonas* (D). A, C, D) scanning electron micrographs; B) polarized light optical micrograph of thin sections of resin-embedded granules.

2.2. Synchrotron micro X-ray fluorescence

μXRF analyses were carried out at the ID21 beamline, at ESRF (Grenoble, France). This beamline is dedicated to X-ray microscopy in the tender X-ray domain (2.0–9.1 keV). For the present experiment, the X-ray energy was set to 2.5 keV (above the sulfur K-edge), using a fixed-exit double-crystal Si(111) monochromator. At this energy, both P and S were simultaneously detected. The XRF signal was collected in the horizontal plane perpendicular to the incident beam direction by using a small-area (30 mm^2) HPGe solid-state energy-dispersive detector, located at 90° with respect to the incident beam. A photodiode was positioned upstream the sample to measure the intensity of the incoming beam. The samples were mounted vertically on a high-precision piezoelectric stage and all the measurements were made under vacuum.

Some measurements were first carried out with a 200 μm unfocussed beam: XRF spectra were collected at 2.5 keV to evaluate the global amount of P and S on a single granule or a set of granules.

Then, to obtain a high lateral resolution elemental mapping, the beam was focused to 0.3 × 0.6 μm^2 using Fresnel zone plates. The samples were raster-scanned horizontally and vertically with respect to the X-ray microprobe, which remained fixed, to produce a two-dimensional image. A photodiode was positioned upstream the sample to measure the intensity of the incoming beam and another one downstream the sample to measure the transmitted signal. Qualitative phase contrast maps were obtained by inserting a pinhole between the sample and this photodiode, slightly off-axis. This simple set-up is very sensitive to phase shift and allows highlighting edge structures of light samples.

The quantitative determination of elemental concentrations is far beyond the scope of the present paper. This is extremely challenging due to strong absorption and re-absorption effects in this energy range (1–2.5 keV) and would require a dedicated effort for the fine calibration of the detection system, as well as the determination of the sample thickness and density. XRF spectra were fitted using the PyMca software package [30], in particular to separate the different contributions from P, S and scattering peaks. Peak areas calculated from the fit were then normalized by the intensity of the incident beam. Results are given with arbitrary units. This allows correcting the variation of the flux of the incoming beam as well as the different dwell times. Accordingly, for similar composition and thickness, results can be directly compared from one grain to another and one map to another.

3. Results and discussion

3.1. Global S and P contents in unfocussed mode

The measurements were first carried out on the bigger starch granules, i.e., those from maize and potato, to evaluate the level of response from such samples. Mutant maize and antisense potato starches lacking GBSS1 (*wx* maize) and phosphorylating enzyme (asGWD), respectively, were used to get very discriminating responses in S and P, respectively. XRF spectra acquired on five starch samples exhibit obvious differences of S and P contents (emission lines at 2.3 and 2.04 keV, respectively) (Fig. 2A).

This shows, in particular, the relatively high concentration of P in WT potato, as well as the high concentration of S in WT maize. A qualitative analysis can be done by comparing the fitted S and P peak intensity (Fig. 2B). Table 1 summarizes the fit results, using the asGWD potato S peak for normalization.

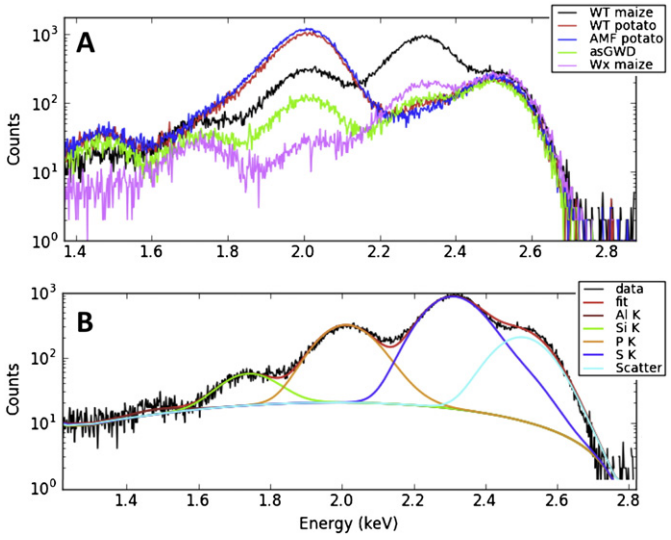

Fig. 2. XRF analysis of 5 different types of starch (WT maize, *wx* maize, *amf* potato, asGWD and WT potato): A) XRF spectra; B) an example of fit using PyMca.

The amount of sulfur is 5 times higher in WT maize when compared to the *waxy* null mutant, which does not contain GBSS1. This confirms the very preliminary results obtained by tryptophan fluorescence on maize starch using synchrotron UV radiation [18]. However a sulfur signal was still obtained with the *wx* maize starch indicating that proteins other than GBSS1 are bound to the polysaccharide including starch-metabolizing enzymes such as SS1 and SBEIIb but also zeins that basically adhere to the surface of the granule [31]. The higher S signal of *wx* maize compared to WT potato is in good agreement with previous biochemical characterization indicating that the level of starch granule bound proteins is higher in maize compared to potato [32].

The P amount in the GWD potato antisense line is 10 times lower than that in WT potato starch, which agrees with the strong decrease in starch-phosphorylating enzyme GWD due to the expression of an antisense construction of the encoding cDNA. These data agree with the phosphate content reported by Blennow et al. [33], i.e.: 3.1 ± 0.3 and 32.1 ± 0.6 nmol/mg starch for asGWD and WT potato starch, respectively.

Similar results were obtained on model plant (*Arabidopsis*) and algal (*Chlamydomonas*) starches (Table 2). The S content determined for GBSS1 mutants is 3 times lower than that in the wild type. The phosphate content is 10 times lower in *Arabidopsis* mutant for GWD (*sex1-3*) than that in the wild type. It has the same value for WT *Chlamydomonas* and the *sta4-2* mutant deficient in a plastidial starch-phosphorylase which mostly influences the rate of starch production but apparently not the phosphorus content. Moreover, a recurrent difference was observed between *Chlamydomonas* starches prepared from strains cultivated under exponential growth conditions (i.e., nitrogen supplied medium (+N) implying active cell-division) or nitrogen starvation (−N; arrested cell-division mimicking storage starch) whatever the genetic background considered: wild type or *sta4-2* mutant. The phosphorus response was much higher when algae were grown in −N conditions (Table 3), which induced massive starch accumulation in the cells [26]. The biological significance of this increase in P content with starch accumulation is not known. Starch accumulation in *Chlamydomonas* cells grown under nitrogen starvation mimics that of long-term storage starch accumulation in seeds or tubers (starch accumulation may occur over several weeks during organs development). Such storage starch is degraded during seed germination or tuber sprouting, releasing carbon and energy required for plant development. Conversely, starch metabolism in *Chlamydomonas* cells cultivated with a source of nitrogen mimics that of transitory starch accumulated in plant source tissues (such as leaves). Transitory starch is submitted to repeated and rapid degradation upon the day–night cycle and it has been shown that starch phosphorylation mostly occurs during degradation at night in *Chlamydomonas* cells and potato leaves [34]. It is likely that the higher P content measured in the nitrogen starved growth condition is a consequence of the extended period of starch accumulation not submitted to recurrent cycles of synthesis-degradation over a relatively short time. Note that such long-term storage starch is also enriched in amylose (25–30% of the starch dry weight; +N starch contains less than 10% amylose). Although phosphorylation is restricted to amylopectin [33] the phosphate content is apparently not negatively correlated to the amylose content of starch. Both processes seem to be distinct.

Table 1
Normalized XRF intensity of P and S on 5 different starch samples (arbitrary units).

	WT potato	asGWD potato	*amf* potato	WT maize	*wx* maize
P	2.64	0.28	3.05	0.80	0.05
S	0.18	0.27	0.11	2.36	0.48

Table 2
Normalized XRF intensity of P and S on *Arabidopsis* and *Chlamydomonas* starch (wild type WT) and mutant deficient in GBSS1 (*gbss1-* and *sta2-* respectively) or starch dikinase (*sex1-3*) or starch phosphorylase (*sta4-*) (arbitrary units).

	Arabidopsis thaliana			*Chlamydomonas reinhardtii*		
	WT	*gbss1-*	*sex1-3*	WT	*sta2-*	*sta4-*
P	0.68	1.05	0.07	0.59	2.16	3.41
S	0.64	0.23	0.59	3.73	0.21	0.46

3.2. Phosphorus and sulfur mapping in single starch granules

With a beam size of approximately $0.3 \times 0.6\ \mu m^2$, S and P were mapped at 2.5 keV in individual granules. For potato starch which contains the biggest starch granules, 5 μm-thick sections were preferred to whole granules to prevent averaging over the total thickness. Maize, *Arabidopsis* and *Chlamydomonas* whole starch granules were mapped directly without sectioning. Maize starch granules are smaller than potato starch granules and polyhedral, which allowed collecting specific information from the peripheral layers of the granule. Granules from *Arabidopsis* and *Chlamydomonas* are much smaller (1 to 5 μm), and it was quite challenging to map such samples and get relevant information from only 5 − 10 pixels per particle.

3.2.1. Phosphorus and sulfur location in potato starch sections (wild type and amylose-free mutant)

Fig. 3 shows the location of phosphorus in sections of potato starch granules, for both the wild type (Fig. 3A) and the amylose-free (*amf*) mutants (Fig. 3B), the latter one being deficient in GBSS1.

In WT potato, phosphorus stemming from phosphate groups is located on the more external layers of the starch granules while it is more homogeneously distributed over the entire granule for the *amf* mutant, which was found to have a higher relative amount of P (Table 1 and Fig. 3). This specific location which has never been shown before is in good agreement with the knowledge that the peripheral regions of the potato starch granules are more crystalline and better organized than in the center [35,36], and that the phosphate groups have to be present in the starch crystalline areas to make them degradable by the degrading enzymes in the starch metabolic cycle. Moreover, Blennow et al. [33] have shown that only amylopectin, which is also considered to be responsible for the semicrystalline architecture of starch, is phosphorylated. Therefore, our results could show that the fraction of amylopectin is preferentially distributed at the periphery of the granule, while that of amylose is mostly present in the center. This new result is particularly interesting in terms of starch structure and biosynthesis. On the contrary, the *amf* mutant, which only contains amylopectin, has phosphate groups distributed over the entire granule. Some attempts to visualize phosphorus have been made by Blennow et al. [17] using PIXE but the experiments were performed on non-sectioned granules and, consequently, the location of the phosphate was averaged through the whole granule.

Fig. 3 also shows the sulfur distribution in potato starch. A lower amount was found in the *amf* mutant in which GBSS1 is lacking while the mapping obtained on WT shows a homogenous distribution of the S signal, suggesting that GBSS1 is homogeneously distributed all over the granule and that other starch granule bound proteins have a negligible impact on S signal. It is the first imaging experiment of GBSS1 in potato starch granule sections, showing that the antisense technique suppresses the expression of the GBSS1 gene and therefore the protein deposition within the granule.

Table 3
Effect of growth conditions on the relative starch phosphorus content of *Chlamydomonas* wild type and *sta4-2* mutant strains. The normalized XRF intensity of P for WT + N is taken as a reference for normalization. +N/−N refer to nitrogen-supplied and nitrogen-starved media, respectively, used for cell culture.

	WT + N	WT − N	*sta4-2* + N	*sta4-2* − N
P	1	26	6	31

3.2.2. S and P mapping in single small starch granules

Scanning the smallest granules (<5 μm) for which only a few pixels were recorded per granule was particularly tricky, especially for the *Chlamydomonas* granules which were definitely too small to detect any distribution feature for P and S, with the present spatial resolution. Fig. 4 shows, as an example, the data recorded for wild-type *Arabidopsis* (Fig. 4A) and the corresponding GWD mutant (*sex1-3*) (Fig. 4B) granules. Although the signal-to-noise ratio is low, it is obvious that the phosphorus response is lower in the mutant, in good agreement with the biochemical data.

S and P maps were also collected on domains enclosing several starch granules as shown for *Arabidopsis ss4-* mutant and WT *Chlamydomonas* and in Fig. 5, the latter being characterized by the accumulation of larger starch granules than in the wild-type [29]. Here again, the lateral resolution was not high enough to generate comprehensive maps of S and P distributions in the granule. The maps recorded on *Arabidopsis ss4-* mutant clearly show that 3–4 μm-large granules are required in order to collect really usable distributions.

3.2.3. S and P amounts in single starch granules

The S and P maps were integrated for each granule to check the granular variability within granules of a given starch source. To prevent from experimental discrepancies between the different maps and scans, like incident flux or recording time, only the S/P ratios were used to compare the different granules. The results were very heterogeneous and, due to the small number and small size of the granules, especially for *Arabidopsis* and *Chlamydomonas*, the statistics were probably not good enough to conclude on inter-granule variability or heterogeneity. Nevertheless, some reproducible S/P peak intensity ratios were found for WT and *amf* potato lines (5 granules) with $0.3 < S/P < 0.5$ and $0.12 < S/P < 0.17$, respectively (Fig. 3). The ratio is lower for the *amf* mutant due to lower content in sulfur. Good results were also obtained for smaller granules, like for example $5.2 < S/P < 7.4$ on 6 granules for the *Arabidopsis ss4-* mutant shown in Fig. 5. This approach represents a very promising alternative to the electron paramagnetic resonance (EPR) method developed by Blennow et al. [33]. This procedure requires the use of Cu^{2+} ions that interact with the phosphate groups inside the starch granule. However, the diffusion of Cu^{2+} could not be controlled and there was no guarantee that the diffusion was homogenous and identical depending on starch origin (which could vary in size, morphology, composition and structure of the forming polysaccharides). The authors concluded that large fractions of the phosphate groups were not exposed for interaction with the copper ions. In addition, Blennow et al. [17] have used PIXE to detect phosphate groups within potato starch granules. However, starch granules were first boiled for 30 min in concentrated HNO_3 before analysis. Therefore, the granule structure was not conserved before analysis. Moreover, only P cartography was possible. In our work, native starch granules or their thin sections were used without any modification that could interfere with the results. Simultaneous imaging of both the granule morphology and high-resolution location of S and P is also very attractive.

4. Conclusion

In this work, synchrotron micro X-ray fluorescence experiments have been performed on starch granules and more generally on endogenous constituents of plants using controlled genetic resources and ultrasmall starch granules purified from model plants. Such experiments have been conducted in previous works mostly on exogenous metals of plants. Here, the focus was to map the trace endogenous elements. Sulfur and phosphorus contents and location within the starch granule are directly connected to important biological issues like starch

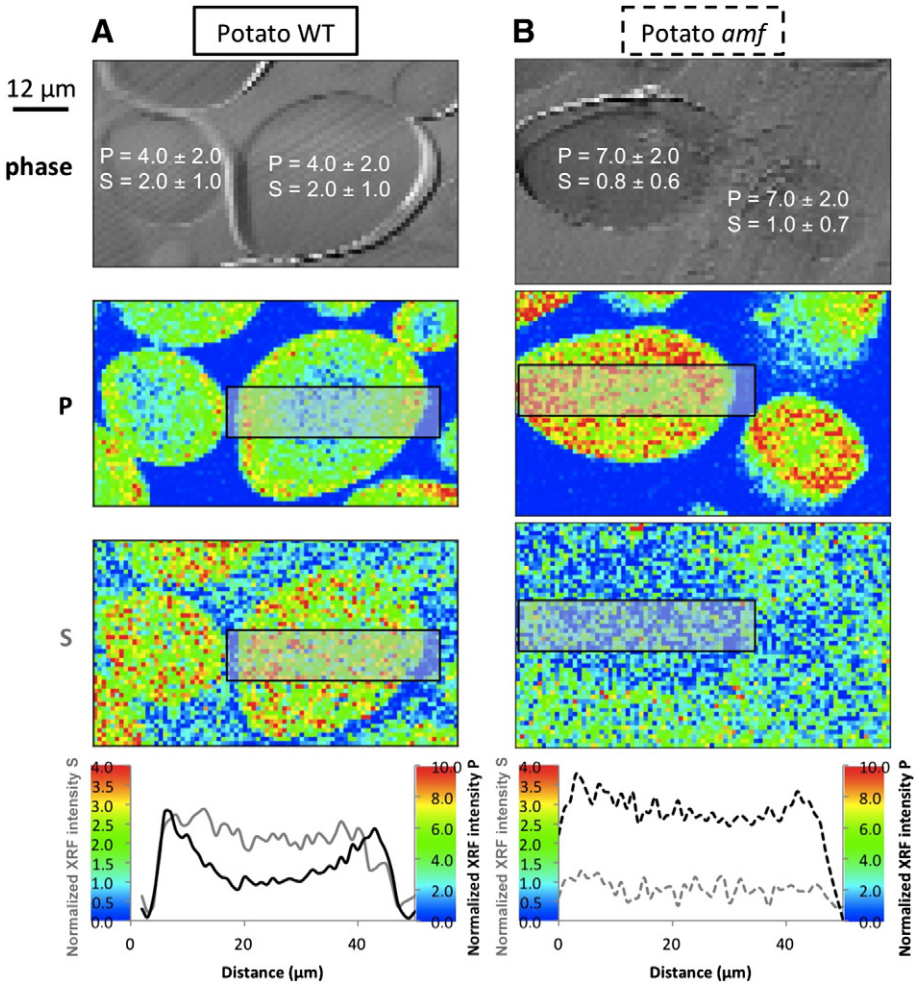

Fig. 3. XRF elemental and phase contrast maps of thin sections of WT (A) and *amf* mutant (B) potato starch. The two starches were sectioned after embedding. On P and S maps, the gray rectangles represent the region where a profile was calculated as an average over 10 µm. Data are presented as normalized XRF intensity for S and P (arbitrary unit), and color scale for the maps is indicated in the profile figures. For the main 2 grains, average and standard deviation of S and P XRF intensities are indicated on the phase map.

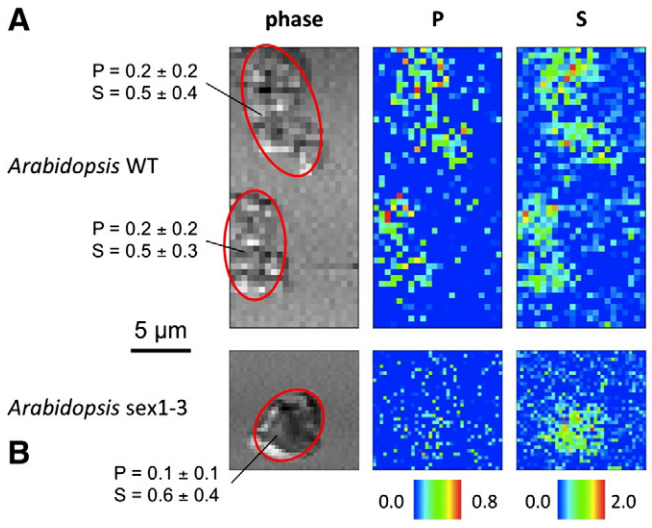

Fig. 4. XRF elemental and phase contrast maps of WT (A) and sex1-3 (B) *Arabidopsis* starch granules. Data are presented as normalized XRF intensity for S and P (arbitrary unit), with the same color scale for the two samples. Average and standard deviation of S and P XRF intensities are indicated on the phase map.

structure and/or metabolism in seeds and leaves. Global measurements of P and S contents in unfocussed mode on series of starch granules of different sources (including mutants for enzymes involved either in phosphorylation or for the major granule-bound enzyme involved in amylose synthesis) allowed the observation of the direct impact of specific biosynthesis schemes. New results were also obtained on the location of P and S in major starch sources like potato and maize and their corresponding amylose-free mutants. These results, especially in terms of mapping, should be confirmed by future thorough experiments, with a specific effort to reach quantitative results. It should open the route to challenging studies on starch biosynthesis, especially during in vitro amylose synthesis that could be performed with purified starch granules impregnated with ADP-glucose, to provide the primary substrate to the amylose-elongating enzyme, the GBSS1.

This study has allowed identifying some experimental constraints especially regarding mapping. For the bigger starch granules, it was necessary to use <5–10 µm-thick sections to prevent from signal averaging over the whole sample thickness. Alternatively, 3D XRF nanotomography may be used to get a complete three-dimensional vision of the element distribution. High-resolution 3D mapping of GBSS1, for example, would lead to a better knowledge of amylose biosynthesis and its location within the starch granule, which are two key questions in the field of starch structure and properties. For granules smaller than 2 µm, nanometric beams are necessary. This would allow taking advantage of important genetic resources available for model starches like those

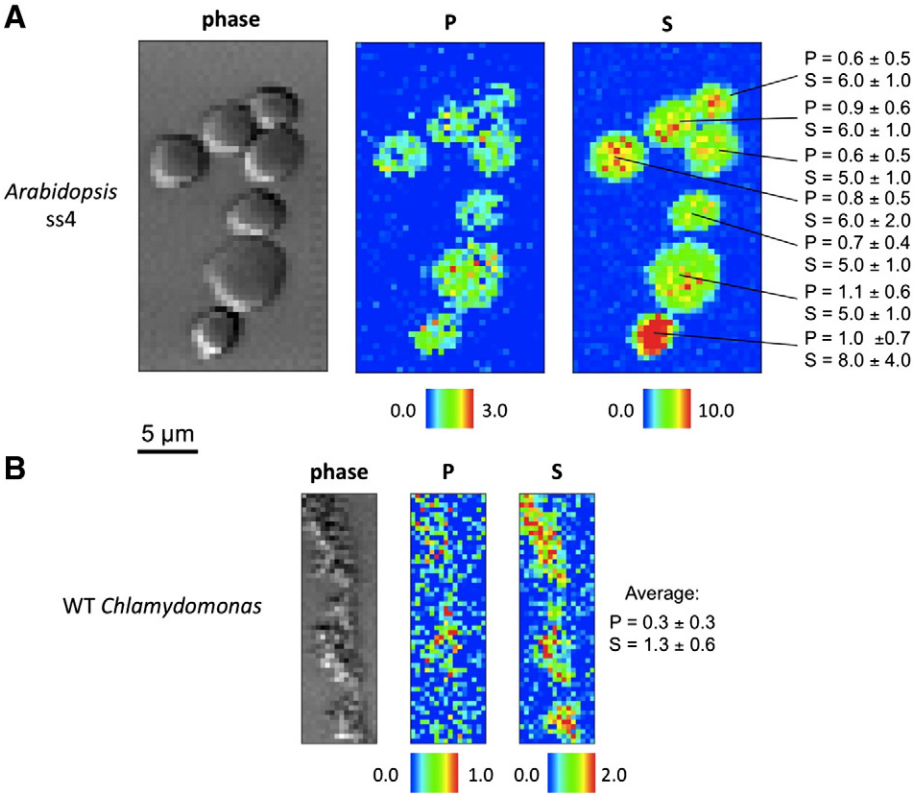

Fig. 5. XRF elemental and phase contrast maps of ultrasmall starch granules from *Arabidopsis ss4*- mutant (A) and WT *Chlamydomonas* (B). Data are presented as normalized XRF intensity for S and P (arbitrary unit). Average and standard deviation of S and P XRF intensities are indicated for single granules for *Arabidopsis* and as a global average for *Chlamydomonas*.

from *Arabidopsis* and *Chlamydomonas*. Such issues will certainly benefit from the nanobeamlines under development at ESRF and other facilities around the world.

Acknowledgements

The experiments were conducted with the financial support of ESRF (proposal SC-2367). The authors thank A. Blennow (University of Copenhagen, Denmark) for giving asGWD potato starch, M. Steup (University of Potsdam, Germany) for *Arabidopsis* starch, P. Mongondry (Engineer School of Agriculture, Angers, France) for thin sections of potato starch, and D. Dupeyre (CERMAV) for SEM images of starch granules.

References

[1] A. Buléon, P. Colonna, V. Planchot, S. Ball, Starch granules: structure and biosynthesis, Int J Biol Macromol 23 (1998) 85–112.
[2] S. Pérez, E. Bertoft, The molecular structures of starch components and their contribution to the architecture of starch granules: a comprehensive review, Starch/Stärke 62 (2010) 389–420.
[3] M. van de Wal, C. D'Hulst, J.-P. Vincken, A. Buléon, R. Visser, S. Ball, Amylose is synthesized in vitro by extension of and cleavage from amylopectin, J Biol Chem 273 (1998) 22232–22240.
[4] F. Wattebled, A. Buléon, B. Bouchet, J.-P. Ral, L. Liénard, D. Delvallé, S. Ball, C. D'Hulst, Granule-bound starch synthase I. A major enzyme involved in the biogenesis of B-crystallites in starch granules, Eur J Biochem 269 (2002) 3810–3820.
[5] N.J. Atkin, S.L. Cheng, R.M. Abeysekera, A.W. Robards, Localisation of amylose and amylopectin in starch granules using enzyme-gold labelling, Starch/Stärke 51 (1999) 163–172.
[6] X.Z. Han, B.R. Hamaker, Location of starch granule-associated proteins revealed by confocal laser scanning microscopy, J Cereal Sci 35 (2002) 109–116.
[7] M. Yusuph, R.F. Tester, R. Ansell, C.E. Snape, Composition and properties of starches extracted from tubers of different potato varieties grown under the same environmental conditions, Food Chem 82 (2003) 283–289.
[8] C.Y. Tsai, The function of the waxy locus in starch synthesis in maize endosperm, Biochem Genet 11 (1974) 83–96.
[9] J.H. Hovenkamp-Hermelink, E. Jacobsen, A.S. Ponsteins, R.G. Visser, G.H. Vos-Scheperkeuter, E.W. Bijmolt, J.N. Vries, B. Witholt, W.J. Feenstra, Isolation of an amylose-free mutation of the potato (*Solanum tuberosum* L.), Theor Appl Genet 75 (1987) 217–221.
[10] K. Denyer, L.M. Barber, R. Burton, C.L. Hedley, C.M. Hylton, S. Johnson, D.A. Jones, J. Marshall, A.M. Smith, H. Tatge, K. Tomlinson, T.L. Wang, The isolation and characterization of novel low-amylose mutants of *Pisum sativum*, Plant Cell Environ 18 (1995) 1019–1026.
[11] A. Blennow, A.M. Bay-Smidt, C.E. Olsen, B. Moller, The distribution of covalently bound phosphate in the starch granule in relation to starch crystallinity, Int J Biol Macromol 27 (2000) 211–218.
[12] A. Blennow, S.B. Engelsen, T.H. Nielsen, L. Baunsgaard, R. Mikkelsen, Phosphorylation of transitory starch is increased during degradation, Trends Plant Sci 7 (2002) 445–450.
[13] J. Fettke, M. Hejazi, J. Smirnova, E. Hochel, M. Stage, M. Steup, Eukaryotic starch degradation: Integration of plastidial and cytosolic pathways, J Exp Bot 60 (2009) 2907–2922.
[14] G. Ritte, J.R. Lloyd, N. Eckermann, A. Rottmann, J. Kossmann, M. Steup, The starch-related R1 protein is an alpha-glucan, water dikinase, Proc Natl Acad Sci U S A 99 (2002) 7166–7171.
[15] L. Baunsgaard, H. Lütken, R. Mikkelsen, M.A. Glaring, T.T. Pham, A. Blennow, A novel isoform of glucan, water dikinase phosphorylates pre-phosphorylated alpha-glucans and is involved in starch degradation in *Arabidopsis*, Plant J 41 (2005) 595–605.
[16] O. Kotting, K. Pusch, A. Tiessen, P. Geigenberger, M. Steup, G. Ritte, Identification of a novel enzyme required for starch metabolism in *Arabidopsis* leaves. The phosphoglucan, water dikinase, Plant Physiol 137 (2005) 242–252.
[17] A. Blennow, A. Sjotland, R. Andersson, P. Kristiansson, The distribution of elements in the native starch granule as studied by particle-induced X-ray emission and complementary methods: notes & tips, Anal Biochem 347 (2005) 317–329.
[18] G. Tawil, F. Jamme, M. Refregiers, A. Vikso-Nielsen, P. Colonna, A. Buléon, In situ tracking of enzymatic breakdown of starch granules by synchrotron UV fluorescence microscopy, Anal Chem 83 (2011) 989–993.
[19] A. Buléon, D.J. Gallant, B. Bouchet, G. Mouille, C. D'Hulst, J. Kossman, S. Ball, Starches from A to C (*Chlamydomonas reinhardtii* as a model microbial system to investigate the biosynthesis of the plant amylopectin crystal), Plant Physiol 115 (1997) 949–957.
[20] N. Van den Koornhuyse, N. Libessart, B. Delrue, C. Zabawinski, A. Decq, A. Iglesias, A. Carton, J. Preiss, S. Ball, Control of starch composition and structure through substrate supply in the monocellular alga *Chlamydomonas reinhardtii*, J Biol Chem 271 (1996) 16281–16287.
[21] C. Zabawinski, N. Van Den Koornhuyse, C. D'Hulst, R. Schlichting, C. Giersch, B. Delrue, C. D'Hulst, J.-M. Lacroix, J. Preiss, S. Ball, Starchless mutants of

Chlamydomonas reinhardtii lack the small subunit of a heterotetrameric ADP-glucose pyrophosphorylase, J Bacteriol 183 (2001) 1069–1077.
[22] B. Delrue, T. Fontaine, F. Routier, A. Decq, J.M. Wieruszeski, N. Van Den Koornhuyse, M.L. Maddelein, B. Fournet, S. Ball, Waxy *Chlamydomonas reinhardtii*: monocellular algal mutants defective in amylose biosynthesis and granule-bound starch synthase accumulate a structurally modified amylopectin, J Bacteriol 174 (1992) 3612–3620.
[23] T. Fontaine, C. D'Hulst, M. Maddelein, F. Routier, T. Pepin, A. Decq, J. Wieruszeski, B. Delrue, N. Van den Koornhuyse, J. Bossu, Toward an understanding of the biogenesis of the starch granule. Evidence that *Chlamydomonas* soluble starch synthase II controls the synthesis of intermediate size glucans of amylopectin, J Biol Chem 268 (1993) 16223–16230.
[24] G. Mouille, M.L. Maddelein, N. Libessart, P. Talaga, A. Decq, B. Delrue, S. Ball, Preamylopectin processing: A mandatory step for starch biosynthesis in plants, Plant Cell 8 (1996) 1353–1366.
[25] D. Dauvillée, V. Chochois, M. Steup, S. Haebel, N. Eckermann, G. Ritte, J.-P. Ral, C. Colleoni, G. Hicks, F. Wattebled, P. Deschamps, C. d'Hulst, L. Liénard, L. Cournac, J.-L. Putaux, D. Dupeyre, S.G. Ball, Plastidial phosphorylase is required for normal starch synthesis in *Chlamydomonas reinhardtii*, Plant J 48 (2006) 274–285.
[26] S.G. Ball, L. Dirick, A. Decq, J.C. Martiat, R. Matagne, Physiology of starch storage in the monocellular alga *Chlamydomonas reinhardtii*, Plant Sci 66 (1990) 1–9.
[27] S. Streb, S.C. Zeeman, Starch Metabolism in *Arabidopsis*, The *Arabidopsis* Book, 2012. e0160.
[28] R. Lorberth, G. Ritte, L. Willmitzer, J. Kossmann, Inhibition of a starch-granule-bound protein leads to modified starch and repression of cold sweetening, Nat Biotechnol 16 (1998) 473–477.
[29] I. Roldán, F. Wattebled, M. Mercedes Lucas, D. Delvallé, V. Planchot, S. Jiménez, R. Pérez, S. Ball, C. d'Hulst, A. Mérida, The phenotype of soluble starch synthase IV defective mutants of *Arabidopsis thaliana* suggests a novel function of elongation enzymes in the control of starch granule formation, Plant J 49 (2007) 492–504.
[30] V.A. Sole, E. Papillon, M. Cotte, P. Walter, J. Susini, A multiplatform code for the analysis of energy-dispersive X-ray fluorescence spectra, Spectrochim Acta B 62 (2007) 63–68.
[31] C. Mu-Forster, B.P. Wasserman, Surface Localization of zein storage proteins in starch granules from maize endosperm. Proteolytic removal by thermolysin and in vitro cross-linking of granule-associated polypeptides, Plant Physiol 116 (1998) 1563–1571.
[32] G.H. Vos-Scheperkeuter, W. de Boer, R.G.F. Visser, W.J. Feenstra, B. Witholt, Identification of granule-bound starch synthase in potato tubers, Plant Physiol 82 (1986) 411–416.
[33] A. Blennow, K. Houborg, R. Andersson, E. Bidzinska, K. Dyrek, M. Labanowska, Phosphate positioning and availability in the starch granule matrix as studied by EPR, Biomacromolecules 7 (2006) 965–974.
[34] G. Ritte, A. Scharf, N. Eckermann, S. Haebel, M. Steup, Phosphorylation of transitory starch is increased during degradation, Plant Physiol 135 (2004) 2068–2077.
[35] D. Gallant, B. Bouchet, A. Buléon, S. Pérez, Physical characteristics of starch granules and susceptibility to enzymatic degradation, Eur J Clin Nutr 46 (1992) S3–S16.
[36] A. Buléon, B. Pontoire, C. Riekel, H. Chanzy, W. Helbert, R. Vuong, Crystalline ultrastructure of starch granules revealed by synchrotron radiation microdiffraction mapping, Macromolecules 30 (1997) 3952–3954.